Low Permeability of Liposomal Membranes Composed of Bipolar Tetraether Lipids from Thermoacidophilic Archaebacterium *Sulfolobus acidocaldarius*†

Hiroaki Komatsu and Parkson Lee-Gau Chong*

Department of Biochemistry, Temple University School of Medicine, Philadelphia, Pennsylvania 19140

Received August 29, 1997; Revised Manuscript Received October 23, 1997⊗

ABSTRACT: The physical origin of the extremely high thermal stability of tetraether liposomes composed of the polar lipid fraction E (PLFE) from the thermoacidophilic archaebacterium *Sulfolobus acidocaldarius* has been investigated. The leakage rate of trapped 5,6-carboxyfluorescein (5(6)CF) and the proton permeability in PLFE liposomes have been measured using fluorescence probe techniques in the temperature range of 25−85 °C. The results are compared with those obtained from nonarchaebacterial liposomes. Egg yolk phosphatidylglycerol (eggPG) and PLFE liposomes exhibit similar large negative zeta-potentials (−31 to −34 mV) and low permeability coefficients for 5(6)CF, indicating that membrane surface charge is responsible for the low leakage rate of 5(6)CF in PLFE liposomes. This assertion is confirmed by the observation of an increased leakage rate of 5(6)CF with decreasing membrane surface negative charge via varying the content of egg yolk phosphatidylcholine (eggPC) in eggPC/eggPG binary mixtures. Gel-state dipalmitoylphosphatidylcholine bilayers and PLFE liposomes exhibit similar permeability coefficients for 5(6)CF, suggesting that lipid packing also plays an important role in the low leakage rate of 5(6)CF. PLFE liposomes, especially those ∼60 nm in diameter, are remarkably thermally stable in regard to proton permeability, which increases by less than 2×10^{-10} cm/s from 25 to 82 °C. The proton permeability comparison of various liposomes reveals that the tight and rigid lipid packing is the major contributor of the extremely low proton permeation in PLFE liposomes; the inositol moiety and the branched methyl groups may also contribute, but to a much lesser extent.

The plasma membrane of thermoacidophilic archaebacterium *Sulfolobus acidocaldarius* mainly consists of bipolar tetraether lipids (∼90% of the total lipid), with the polar lipid fraction E (PLFE)[1] as the major component (*1*). This fraction contains a mixture of tetraether lipids with either a glycerol dialkyl nonitol tetraether (GDNT) or a glycerol dialkyl glycerol tetraether (GDGT) skeleton (Figure 1). GDNT (∼90% of total PLFE lipids) has phosphatidylmyoinositol on one end and β-glucose on the other, whereas GDGT (∼10%) has phosphatidylmyoinositol attached to one glycerol and β-D-galatosyl-D-glucose to the other glycerol backbone (*1*−*4*) (Figure 1). Each of the biphytanyl hydrocarbon chains in the PLFE lipids contains up to four cyclopentane rings, and the number of cyclopentane rings increases with increasing growth temperature (*5*).

PLFE lipids are the only polar lipid fraction from *S. acidocaldarius* known to form closed and stable multilamellar and unilamellar liposomes in aqueous solutions (*1*, *6*). For this reason, PLFE liposomes have been used as a model system for studying *S. acidocaldarius* archaebacterial membranes. Electron microscopic analysis indicated that, in PLFE liposomes, the lipids span the entire lamellar structure, forming a monomolecular thick membrane (*6*). Fluorescence (*7*) and differential scanning calorimetric (E. Chang, personal communication) studies did not detect any distinct thermal- or pressure-induced phase transitions in PLFE liposomes in the pressure and temperature ranges of 0.001−1.5 kbar and 5−90 °C.

PLFE liposomes possess remarkable thermal stability. The lateral mobility of the pyrene-labeled phosphatidylcholine in PLFE liposomes was found to be highly restricted, as compared to nonarchaebacterial lipid membranes, and started gaining some lateral mobility only for temperatures higher than 48 °C (*7*). The thermal stability of PLFE liposomes was also studied in terms of leaks of markers from the inner aqueous compartment of the liposome to the bulk aqueous phase. By monitoring the leakage of 6-carboxyfluorescein originally trapped inside the vesicle, Chang (*8*) found that PLFE liposomes exhibit unusual thermal stability up to at least 80 °C and are less permeable to 6-carboxyfluorescein than nonarchaebacterial lipid membranes such as 1-palmitoyl-2-oleoyl-L-α-phosphatidylcholine (POPC) and diphytanoyl-L-α-phosphatidylcholine (DPhPC) at the temperatures (5−60 °C) examined. Using 6-carboxyfluorescein and pyranine as the markers, Elferink et al. (*9*) reported increased thermostability in the liposomes prepared from *S. acidocaldarius* tetraether lipids, as compared to the liposomes

† This work was supported by a grant from the NSF (MCB-9513669).

* To whom correspondence should be addressed.

⊗ Abstract published in *Advance ACS Abstracts,* December 15, 1997.

[1] Abbreviations: PLFE, polar lipid fraction E; LUVET, large unilamellar vesicles made by the extrusion technique; SUVET, small unilamellar vesicles made by the extrusion technique; PC, phosphatidylcholine; DPPC, dipalmitoyl-L-α-phosphatidylcholine; DSPC, distearoyl-L-α-phosphatidylcholine; eggPC, egg yolk L-α-phosphatidylcholine; eggPG, egg yolk L-α-phosphatidylglycerol; SoyPI, soybean L-α-phosphatidylinositol; GDNT, glycerol dialkylnonitol tetraether; GDGT, glycerol dialkylglycerol tetraether; DPhPC, diphytanoyl-L-α-phosphatidylcholine; 5(6)CF, 5,6-carboxyfluorescein.

S0006-2960(97)02163-6 CCC: $15.00
Published on Web 01/06/1998

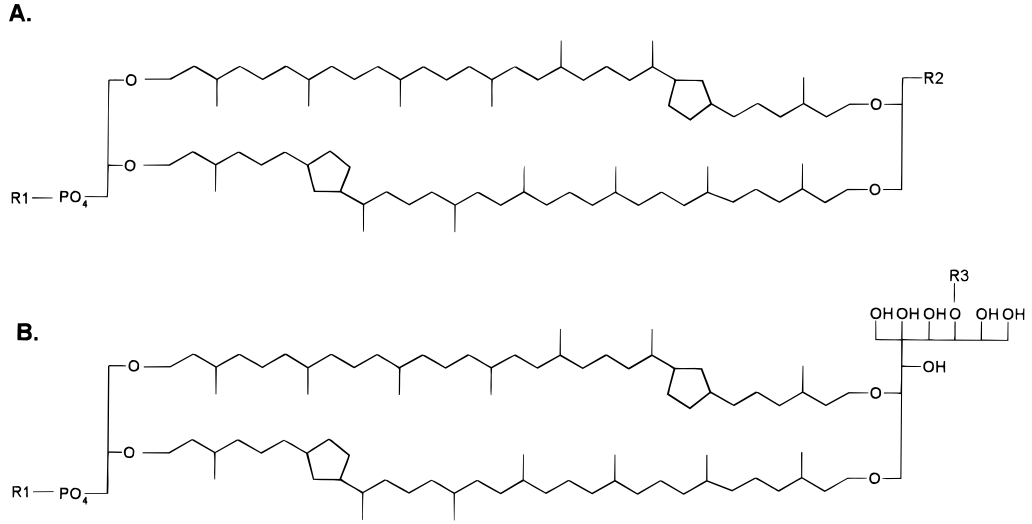

FIGURE 1: Structures of PLFE lipids: (A) glycerol dialkylglycerol tetraether (GDGT) and (B) glycerol dialkylnonitol tetraether (GDNT). R1 = inositol; R2 = β-D-glucopyranose; and R3 = β-D-galactosyl-β-D-glucopyranose. The number of cyclopentane rings can vary from 0 to 4 in each phytanyl chain (*5*) (adopted from ref 1).

composed of diester lipids from the mesophilic bacterium *Escherichia coli* or the thermophilic bacterium *Bacillus stearothermophilus*. In addition, the thermal stability of PLFE liposomes was investigated in terms of proton permeation from the bulk aqueous phase toward the interior of the liposome. Elferink et al. (*9*) demonstrated that the proton permeability in PLFE liposomes is lower and less temperature sensitive than that in liposomes composed of diester lipids from *E. coli* or *B. stearothermophilus*. These studies provide partial explanations for why *S. acidocaldarius* can sustain high growth temperatures (e.g., 59−100 °C) and live in acidic environments (e.g., pH 2.5) (*10*) while the intracelluar compartment is maintained at pH 6.5. The unusual thermal stability also makes PLFE tetraether liposomes attractive for applications in biotechnology (*11*) such as the development of drug delivery systems.

However, to date, the origin of the unusual thermal stability of PLFE liposomes remains unclear. Chang (*8*) and Elferink et al. (*9*) reported that the stability of PLFE liposomes with respect to 6-carboxyfluorescein leakage is not due to the phytanyl structure of the hydrocarbon chain, in contrast to the perception of Yamauchi et al. (*12*). Elferink et al. (*9*) proposed that the low proton permeability of PLFE liposomes is a consequence of the chemical structure of the lipids, due to the network of hydrogen bonds between the sugar residues of PLFE exposed at the outer face of the membrane, but this proposition has not been tested experimentally.

In the current work, we have addressed the above issue by conducting a comparative temperature study on the leakage of trapped 5,6-carboxyfluorescein (5(6)CF) and on the proton permeability in PLFE and various nonarchaebacterial liposomes. The resulting permeability coefficients and the zeta-potentials of liposomes have identified that the tight and rigid lipid packing and the negative charges on the membrane surface are responsible for the low leakage rate of 5(6)CF in PLFE liposomes. The proton permeability comparison of various liposomes reveals that the tight and rigid lipid packing is the major contributor of the low proton permeability in PLFE liposomes; the inositol moiety and the branched methyl groups may also contribute, but to a much lesser extent. Our data have also demonstrated that the proton permeability in small PLFE liposomes (~60 nm in diameter) is lower and less temperature sensitive than that in large PLFE liposomes (~240 nm in diameter).

MATERIALS AND METHODS

Materials. PLFE lipids were isolated from *S. acidocaldarius* (strain DSM639 from acid hot spring, ATCC, Rockville, MD) grown aerobically and heterotrophically at 69 °C, pH 2.5, using the method of Lo and Chang (*1*). In brief, dried *S. acidocaldarius* cells were soxhlet-extracted with chloroform/methanol (1:1, v/v) for 24 h. The crude lipids were fractionated by reversed-phase column chromatography using C-18 PrepSep columns (Fisher Scientific, Fair Lawn, NJ) eluted first with methanol:water (1:1, v/v) (filtrate A) and then with chloroform:methanol:water (0.8:2:0.8, v/v/v) (filtrate B). Filtrate B was further separated by thin-layer chromatography (TLC) eluted with chloroform:methanol:water (65:25:4, v/v/v). The PLFE fraction ($R_f \approx 0.2$) was scraped from silica TLC plates and eluted with chloroform:methanol:water (1:2:0.8, v/v/v). Finally, PLFE was purified by cold methanol precipitation two to three times.

Dipalmitoyl L-α-phosphatidylcholine (DPPC), distearoyl L-α-phosphatidylcholine (DSPC), egg yolk L-α-phosphatidylcholine (eggPC; acyl compositions: 16:0 (34%), 16:1 (1%), 18:0 (11%), 18:1 (31%), 18:2 (18%), 20:4 (3%), and others (2%), according to the manufacturer's analysis), soybean L-α-phosphatidylinositol sodium salt (SoyPI), and diphytanoyl L-α-phosphatidylcholine (DPhPC) were obtained from Avanti Polar Lipids (Alabaster, AL). 5(6)CF and egg yolk L-α-phosphatidylglycerol sodium salt (eggPG; acyl compositions: 16:0 (33%), 16:1 (1%), 18:0 (13%), 18:1 (30%), 18:2 (15%), 20:4 (2%), and others (4%), according to the manufacturer's analysis), cholesterol, and valinomycin were purchased from Sigma (St. Louis, MO).

Liposome Preparation. The stock solution of PLFE was prepared in chloroform/methanol/water (65:25:4, v/v/v). Stock solutions of other lipids were prepared in chloroform/ethanol (99:1, v/v) and kept at −20 °C under nitrogen prior to use. Aliquots of the lipid stock solutions were dried in a

cryogenic vial under nitrogen and then left under vacuum for at least 12 h. For 5(6)CF leakage measurements, 0.4 mL of 42 mM 5(6)CF buffer (185 mosM, pH 7.6) was added to the dried lipids. For proton permeability measurements, 0.4 mL of 5 mM 5(6)CF in 50 mM sodium pyrophosphate/citrate buffer (pH 7.0) was added to the lipids. The vial was flushed with nitrogen and then sealed. The lipids were hydrated at 70 °C for PLFE and at 25 °C for eggPC, eggPC/cholesterol (7/3 in molar ratio), DPhPC, eggPG, and SoyPI. For other lipids, the hydration temperature was 10 °C above their gel-to-liquid-crystalline phase transition temperatures.

5(6)CF-entrapped unilamellar vesicles were made by freezing-thawing and extrusion methods (*13*). In brief, liposome dispersions were obtained by freezing in dry ice/ethanol and thawing at the hydration temperature as described above. The freezing-thawing cycle was repeated five times. Liposomes were then extruded five times using a lipid extruder (Lipex, Vancouver, Canada) through two stacked 0.05 μm or 0.2 μm polycarbonate membranes under 4000 or 2000 kPa nitrogen gas pressure, respectively, at the same temperatures as those used for the hydration. The free 5(6)-CF molecules were removed by a Sephadex G-50 column using 50 mM sodium pyrophosphate/citric acid buffer (185 mosM, pH 7.0 or 7.6) as an eluent at ~24 °C. The large and small vesicles extruded through the filter of 0.05 or 0.2 μm pore size are designated as SUVETs and LUVETs, respectively.

Characterization of Liposomes. Average diameters of the obtained liposomes, with 42 mM 5(6)CF entrapped in the inner aqueous compartment, were estimated as a light-intensity average using a dynamic light scattering technique with a Zetasizer-4 photon-correlation spectrometer (Malvern Instruments, Worcs, U.K.). In the peak analysis, the weight-weighted diameters were evaluated as described elsewhere (*14*, *15*).

To estimate zeta-potentials as a measure of the surface potential of the liposomal membranes, dynamic light scattering measurements in combination with an electrophoresis were carried out using the Zetasizer-4 photon-correlation spectrometer. The zeta-potentials were measured at 25 °C using a ZET 5103 small capillary cell in a cross-beam mode, and 100 V was applied in the electrophoresis as described elsewhere (*16*).

Measurements of 5(6)CF Leakage. Leakage of 5(6)CF from the internal liposome compartment to the exterior aqueous phase was measured by the extent of the 5(6)CF fluorescence intensity increase. The rationale is that if 5(6)-CF is trapped inside the liposome at a self-quenched concentration, changes in its concentration due to leakage through the membrane will lead to dequenching and, thus, a higher fluorescence intensity (reviewed in *17*). To initiate this experiment, 10 μL of 5(6)CF-entrapped liposomes in 50 mM sodium pyrophosphate/citrate buffer (pH 7.6) stored at 5 °C was rapidly injected into 3 mL of the same buffer in a fluorescence cuvette preincubated at the desired temperature ranging from 25 to 85 °C. This temperature-jump method (*18*) was used to avoid possible 5(6)CF leakage through the lipid phase transition, at which solute permeation is greatly enhanced via gel−fluid interfaces of lipid clusters (*19*). Immediately after the injection, the fluorescence intensity of 5(6)CF at 516 nm (band-pass = 4 nm) was monitored over time on a SLM DMX-1000 fluorometer (Urbana, IL) using an excitation at 490 nm (band-pass = 1 nm). Samples were stirred during measurements. Final concentrations of lipids in the cuvette were ~12 μM. The concentration of 5(6)CF trapped in the interior of the vesicle was controlled below 0.5 μM. In this concentration region, a linear relationship between the fluorescence intensity and the 5(6)-CF concentration was obtained even when all the 5(6)CF molecules trapped in the inner aqueous compartment were leaked out upon membrane disruption by Triton X-100.

Because leakage of entrapped substances from the inner aqueous compartment of the liposome follows first-order kinetics (*20*), the increase of fluorescence intensity, I, of 5(6)-CF with increasing incubation time t can be described as (*21*)

$$\ln(1 - I/I_{inf}) = C - kt \quad (1)$$

where C is a constant and I_{inf} is the fluorescence intensity after lysis of liposomes using Triton X-100, respectively. The rate constant k can be further related to the permeability coefficient P by the equation (*22*)

$$k = SP/V_i \quad (2)$$

where the surface area S and the inner compartment volume V_i of the liposome can be estimated from liposome sizes.

Measurements of Proton Permeability. When concentrations of 5(6)CF are too low to produce self-quenching, the fluorescence intensity of 5(6)CF is pH-dependent, decreasing about 20% per pH unit over the pH range of 8−5 as the proportion of the ionized species of the 5(6)CF molecules decreases (*23*). Using this property, we have measured the proton permeability (*24*−*26*) in terms of the pH change inside the PLFE or nonarchaebacterial liposomes. Specifically, 3 mL of 50 mM sodium pyrophosphate/citrate buffer (pH 2.5 unless otherwise specified) was incubated in a fluorescence cuvette at the desired temperature for at least 10 min. To this solution were injected 10 μL of 5 mM 5(6)-CF-entrapped liposomes in 50 mM sodium pyrophosphate/citrate buffer (pH 7.0) stored at 5 °C, making the final lipid concentration ~12 μM. The change in fluorescence intensity of 5(6)CF in response to the pH gradient across the membrane was monitored as a function of time on the SLM DMX-1000 fluorometer. The fluorescence intensity was measured, while stirring, at 516 nm (4 nm band-pass) with an excitation at 490 nm (1 nm band-pass). In this experiment, the term "proton permeability" is used for both proton and hydroxide ion permeabilities because we cannot differentiate the proton flux from a counter flux of hydroxide ion (*25*, *27*). In the analysis of the proton permeability, it can be assumed that 5(6)CF initially entrapped in the liposomes does not leak out to the bulk aqueous phase because the permeation rate of 5(6)CF is two orders of magnitude smaller than that of the proton.

RESULTS AND DISCUSSION

5(6)CF Leakage. In general, the plots of $\ln(1 - I/I_{inf})$ vs incubation time t for PLFE and nonarchaebacterial lipid LUVETs are linear (illustrated in Figure 2A), and their slopes allow us to calculate the 5(6)CF leakage rate constant k via eq 1. In order to calculate the permeability coefficient P by eq 2, the average diameters of the liposomes were determined

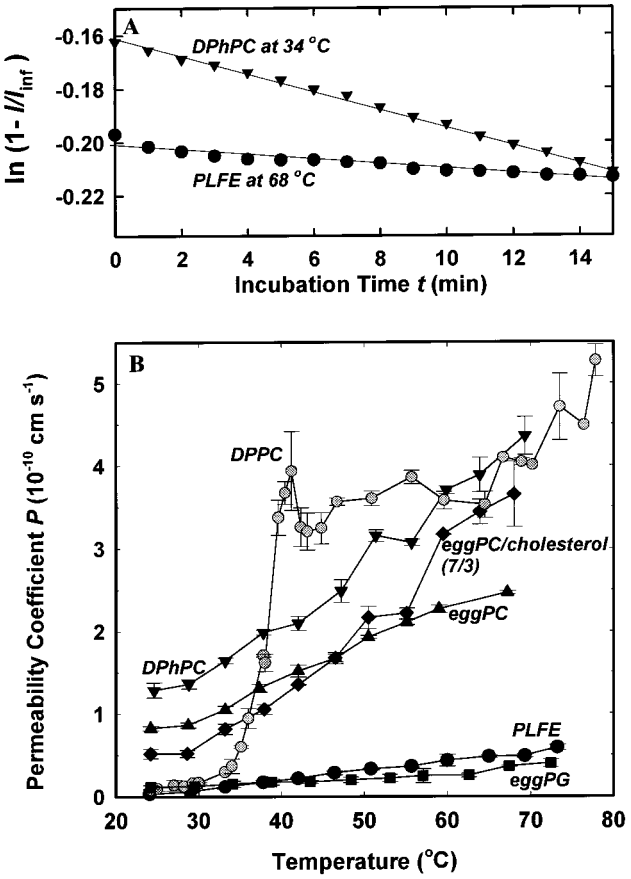

FIGURE 2: (A) Typical plots of $\ln(1 - I/I_{inf})$ vs incubation time t for 5(6)CF leakage in PLFE and nonarchaebacterial LUVETs. (B) Permeability coefficients P of 5(6)CF in various LUVETs as a function of incubation temperature. Plots are average ± S.E. of at least three independent measurements (error bars in other figures bear the same meaning).

by dynamic light scattering, and the results are presented in Table 1. The estimated average diameter of PLFE LUVETs was 240 nm. This value is consistent with those obtained by Chang (*8*) and Elferink et al. (*9*) (234 and 219 nm, respectively) for PLFE liposomes prepared using similar methods. Using the estimated liposome diameters and assuming that the temperature dependence of the liposome size is negligible and that the membrane thickness is small as compared to the diameter, we have calculated permeability coefficients P as a function of incubation temperature. The results are presented in Figure 2B.

The permeability coefficients for PLFE liposomes are significantly lower and less temperature sensitive than those for DPhPC, eggPC, eggPC/cholesterol, and DPPC (>30 °C) liposomes (Figure 2B); this general trend agrees with the work by Chang (*8*). The monotonic increase in P with increasing temperature in PLFE LUVETs (Figure 2B) indicates the lack of lipid phase transition in the temperature range examined, a result consistent with previous findings (*7*). The high P values for DPhPC (Figure 2B) signal that the phytanyl structure *per se* is not responsible for the low permeability of PLFE LUVETs to 5(6)CF.

More interestingly, eggPG and PLFE liposomes exhibit similar low permeability coefficients for 5(6)CF over the entire temperature range examined, whereas eggPG and eggPC exhibit distinct permeability coefficients (Figure 2B). EggPG and eggPC possess similar acyl compositions (see Materials and Methods). Thus, the differences in permeability coefficient between eggPG and eggPC LUVETs (Figure 2B) can only be attributed to something other than generation of lipid fragments by double-bond oxidation. PLFE lipids do not have double bonds in their hydrocarbon chains and would be expected to be highly resistant to lipid oxidation, in contrast to the situation of eggPG. Yet, both eggPG and PLFE liposomes exhibit similar low permeability coefficients for 5(6)CF (Figure 2B). This suggests that a common structural factor between eggPG and PLFE is responsible for the low permeability of 5(6)CF in PLFE LUVETs. Note that, at neutral pH, eggPG and PLFE as well as the entrapped 5(6)CF (but not eggPC) are negatively charged and the repulsive interactions between the negative charges should impede the permeation of 5(6)CF across the membrane. This suggests that membrane surface charge plays a role in the low leakage rate of 5(6)CF in PLFE liposomes, a finding not revealed in previous studies.

The above assertion has been tested by measuring the zeta-potentials of PLFE and eggPG liposomes and by changing the membrane surface charge density via varying the content of eggPC in eggPC/eggPG binary mixtures. As shown in Table 1, the PLFE and eggPG LUVETs display relatively large negative zeta-potentials, −31 to −34 mV, respectively, whereas eggPC LUVETs display a much lower value, −7.5 mV. These results indicate that the surface of PLFE liposomes is rich in negative charges at neutral pH, in a way similar to eggPG liposomes. Figure 3 (open and closed circles) shows that the permeability coefficient of 5(6)CF decreases with increasing content of eggPG in eggPG/eggPC binary mixtures. Figure 3 (squares) also shows that as the content of eggPG in the eggPG/eggPC binary mixtures varies from 0 to 100 mol %, the zeta-potential changes from −7 to −34 mV. It appears that the permeability coefficient of 5(6)-CF is inversely correlated with the extent of negative charges on the membrane surface. This implies that the negatively charged surface of the PLFE liposomes due to the presence of the phosphate groups is, at least partially, responsible for the low permeability of 5(6)CF.

It is interesting to mention that *in vivo* the phosphate groups of archaebacterial tetraether lipids reside mainly on the intracellular side (*9*). Under normal growth conditions, the intracellular pH of *S. acidocaldarius* is ∼6.5. At this pH, the phosphate moiety is negatively charged. The negatively charged layer on the intracelluar side of the plasma membrane should establish a strong barrier to retain anionic metabolites within the cell even at high temperatures such as 59−85 °C, as implied by our data presented in Figures 2B and 3 and Table 1.

Figure 2B also shows that the permeability coefficient P in DPPC LUVETs undergoes an abrupt change from 35 to 40 °C, corresponding to the pretransition and the main transition temperatures of DPPC, respectively. The permeability coefficients for 5(6)CF leakage in the gel-state DPPC bilayers (below 30 °C) are low, similar to those in PLFE LUVETs. It is known that lipid acyl chains in the gel state of DPPC are highly ordered and that the ordered lipid structure decreases solute permeability (*28*). In addition, previous fluorescence probe studies indicated that lipid packing in PLFE liposomes is tight and rigid below 30 °C (*7*, *29*). Tight and rigid lipid packing in PLFE liposomes is also evident from molecular modeling studies (J. Gabriel,

Table 1: Average Sizes, Zeta-Potentials, and Activation Energy E_a for the Leakage of 5(6)CF and the Proton Permeation in a Variety of Liposomes

liposomes	avg diameter[a] (nm) avg ± S.D. ($n = 3-5$)	zeta-potential[b] (mV) avg ± S.D. ($n = 3$)	E_a (kcal/mol) (r)[n] 5(6)CF	proton
PLFE SUVET	60.5 ± 2.1	–	–	6.7 (0.98)
PLFE LUVET	240.2 ± 3.5	−34.3 ± 2.0	20.2[c] (0.96)	5.1 (0.95)
			5.6[d] (0.98)	
with K^+ + Val[h]	–	–	–	9.9 (0.97)
eggPC LUVET	158.6 ± 2.0	−7.5 ± 0.8	6.2 (0.98)	17.0 (0.99)
with K^+ + Val[i]	–	–	–	7.0 (0.94)
eggPC/cholesterol (7/3) LUVET	180.9 ± 1.1	–	9.9 (0.98)	–
eggPG LUVET	158.0 ± 3.1	−31.4 ± 3.1	5.2 (0.96)	8.2 (0.97)
DPhPC LUVET	176.7 ± 2.1	–	5.8 (0.99)	14.5 (0.99)
DPPC LUVET	202.4 ± 3.1	–	21.5[e] (0.96)	–
			68.5[f] (0.98)	
			[g]	
DSPC LUVET	180[m]	–	–	1.4[j] (0.83)
				40.9[k] (1)
				18.4[l] (0.98)
SoyPI LUVET	157.5 ± 1.7	–	–	10.5 (0.98)

[a,b] In 50 mM sodium pyrophosphate/citrate buffer (pH 7.6) at 20 °C. [c] Below 43 °C. [d] Above 43 °C. [e] Below the pretransition temperature (35 °C) of DPPC liposome. [f] Between the pretransition temperature (35 °C) and the main phase transition temperature (41 °C) of DPPC liposome. [g] Above the main phase transition temperature (41 °C) of DPPC liposome, the negative value was obtained. [h,i] In the presence of 50 mM K_2SO_4 and (h) 0.01 μM or (i) 0.05 μM valinomycin, and pHs in the inner and outer phases of the liposomes were 7.0 and 6.0, respectively. [j] Below the pretransition temperature (49 °C) of DSPC liposome. [k] Between the pretransition temperature (49 °C) and the main phase transition temperature (55 °C) of DSPC liposome. [l] Above the main phase transition temperature (55 °C) of DSPC liposome. [m] An assumed value (*13*). [n] Regression correlation coefficient. −, not done.

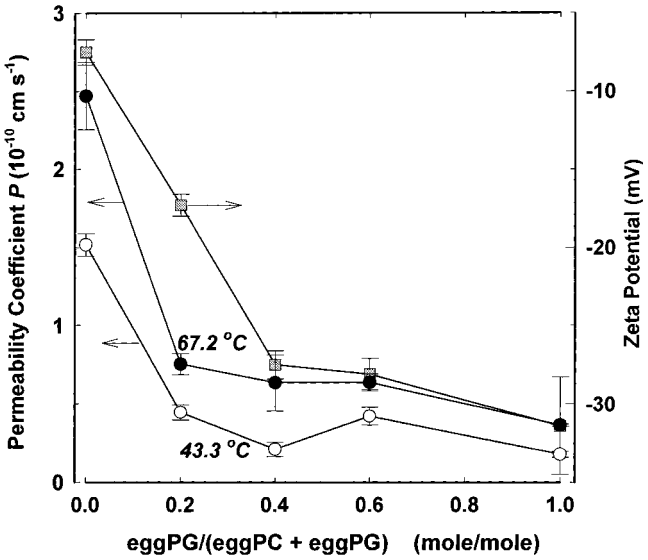

FIGURE 3: Effect of eggPG content on the permeability coefficient P of 5(6)CF in the LUVETs of eggPG/eggPC binary mixtures at two temperatures (open and closed circles) and on their zeta-potentials (squares) measured at 25 °C.

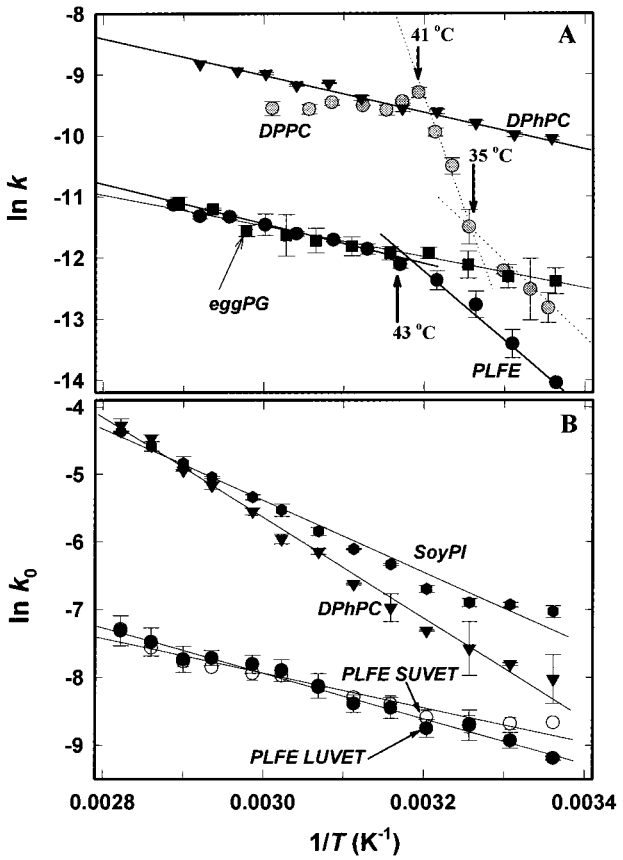

FIGURE 4: Arrhenius plots of (A) 5(6)CF leakage and (B) proton permeation in a variety of liposomes. The lines were related to the data with a regression equation coefficient $r > 0.90$ using Sigma Plot (Jandel Scientific Software, San Rafael, CA).

personal communication). Taken together, the similarity in the permeability coefficient of 5(6)CF leakage between the gel state DPPC bilayers and PLFE LUVETs (Figure 2B) suggests that lipid packing is also of major importance in the low membrane permeability of PLFE liposomes.

The Arrhenius plots of the rate constant of 5(6)CF leakage in eggPG and DPhPC LUVETs are linear (Figure 4A), which is consistent with previous reports of lacking any main phase transition in these (or similar) lipid membranes in the temperature range examined (*30*, *31*). As expected, the Arrhenius plot for DPPC LUVETs exhibits two breakpoints, namely, 35 and 41 °C, which correspond to the pretransition and the main phase transition temperatures of DPPC. The surprising result is that the Arrhenius plot of the rate constant of 5(6)CF leakage in PLFE liposomes displays a breakpoint at ~43 °C (Figure 4A), yielding two activation energies, 20.2 kcal/mol below 43 °C and 5.6 kcal/mol above (Table 1). The presence of two activation energies for leakage of 5(6)-

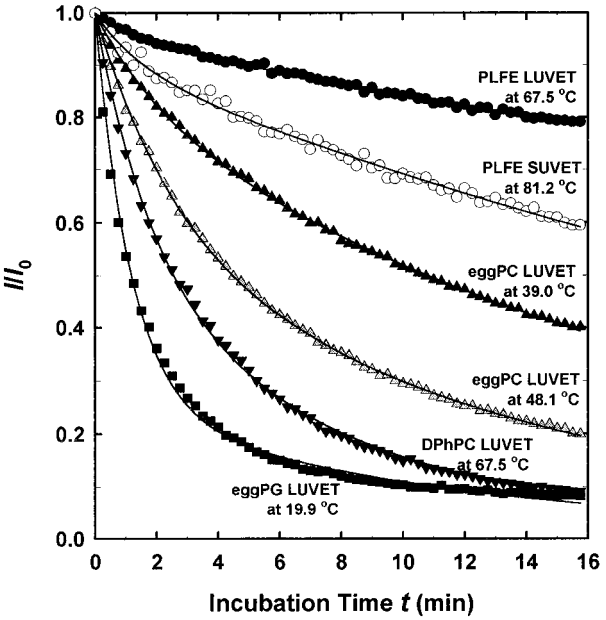

FIGURE 5: Typical plots of fluorescence intensity of 5(6)CF (I/I_0) vs incubation time (t), in response to a pH gradient across the membranes (pH 7.0 in the inner compartment and pH 2.5 outside the liposome) in a variety of LUVETs. Solid lines are the best fit to the equation $I/I_0 = A \exp(-k_1 t) + (1 - A) \exp(-k_2 t)$.

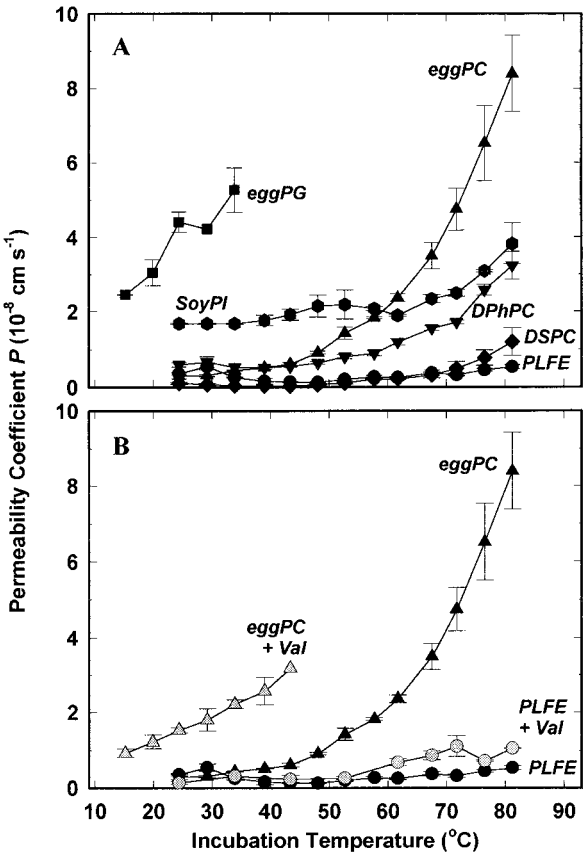

FIGURE 6: Effect of incubation temperature on apparent proton permeability, P, in PLFE LUVETs and in various nonarchaebacterial LUVETs in the absence (A) and presence (B) of valinomycin. The data labeled with eggPC + Val and PLFE + Val were obtained in the presence of 50 mM K_2SO_4 and valinomycin (0.01 μM for eggPC and 0.05 μM for PLFE) using a pH gradient of 1.0 (pH 7.0 in the interior and pH 6.0 in the bulk aqueous phase).

CF across the same PLFE membrane (Table 1) indicates that the energy barrier for transporting the 5(6)CF molecules from the inner compartment of PLFE LUVETs to some sort of "activated" state changes at ~43 °C. Because the activation energies, in general, lack a clear physical meaning, the change in the "activated" state cannot be specified. But, this breakpoint temperature, which was not revealed in the previous study by Chang (*8*), cannot be linked to the bulk lipid phase transition arising from the hydrocarbon region because PLFE liposomes do not exhibit any distinct main phase transition as judged by differential scanning calorimetry and fluorescence probe measurements, as mentioned earlier. However, it is interesting to note that this breakpoint temperature comes close to the onset temperature (48 °C) for the lateral mobility of pyrene-labeled phosphatidylcholine in PLFE liposomes (*7*). Since lipid lateral motion depends on membrane free volume (*32*), the similar values for both the onset temperature in lateral mobility (*7*) and the breakpoint temperature in the Arrhenius plot of 5(6)CF leakage (Figure 4A) suggest that membrane free volume (inferentially, lipid packing) may be involved in the determination of the leakage rate of 5(6)CF in PLFE liposomes, in agreement with the implication derived from the DPPC data (Figure 2B).

Proton Permeability. Typical plots of fluorescence intensity, I, of 5(6)CF at 516 nm vs incubation time, in response to a pH gradient of 4.5 (pH 7.0 inside and pH 2.5 outside the liposome), for a variety of LUVETs and PLFE SUVETs are shown in Figure 5, where I_0 is the fluorescence intensity at time zero. This pH gradient was chosen because it closely resembles the real growth condition for *S. acidocaldarius*, namely, pH 2.5 in the growth medium and pH 6.5 in the intracellular compartment. The fluorescence intensity change over time can be satisfactorily described by a double exponential decay function: $I/I_0 = A \exp(-k_1 t) + (1 - A) \exp(-k_2 t)$. Here, A is the preexponential factor and k_1 and k_2 are rate constants. Using the average rate constant $\langle k \rangle$ ($= Ak_1 + (1 - A)k_2$) or the initial rate constant k_0 and the S and V_i values estimated from liposome size, we have calculated the apparent proton permeability coefficient P via eq 2. The apparent proton permeability coefficients, P, calculated from $\langle k \rangle$, in eggPG, eggPC, SoyPI, DPhPC, DSPC, and PLFE LUVETs as a function of incubation temperature are shown in Figure 6A. Similar results were obtained with the P values calculated from k_0 (data not shown).

The P values of PLFE LUVETs are virtually the lowest among all the liposomes examined, especially at high temperatures. At 65−82 °C, the proton permeability coefficients in PLFE liposomes are as low as $(0.3-0.5) \times 10^{-8}$ cm/s (Figure 6A). This result suggests that bipolar tetraether PLFE lipids alone, without active proton pumps, could play an important role in maintaining an intracellular pH at 6.5 in *S. acidocaldarius* while the growth medium is acidic (pH 2.5). Also, the P values in PLFE liposomes are the least temperature sensitive among all the liposomes examined. From 25 to 82 °C, P in PLFE LUVETs increases only by a factor of 1.4, whereas P in DPhPC, DSPC, and eggPC LUVETs increases by 5.5, 12, and 28 times, respectively. This result indicates that PLFE tetraether liposomes are remarkably thermally stable in regard to proton permeability. A similar conclusion was made previously by Elferink et al. (*9*) on the basis of comparison with diester liposomes from

E. coli and *B. stearothermophilus*. However, because those diester liposomes exhibited proton permeability coefficients 33−65 times higher than PLFE tetraether liposomes from *S. acidocaldarius* at 40 °C (*9*), their comparative study did not allow identification of the structural factors responsible for the low proton permeation in PLFE liposomes.

In our present study, we have compared PLFE liposomes with several simple and well-documented nonarchaebacterial liposomes in an attempt to unravel the physical origin of the low proton permeation found in PLFE LUVETs. EggPG LUVETs exhibit the highest proton permeability among all the liposomes examined (Figure 6A). This indicates that the negative charge on the membrane surface is not the contributing factor for the low proton permeability in PLFE liposomes. The proton permeabilities in DPhPC and SoyPI LUVETs are much smaller than those in eggPG LUVETs but still significantly higher than those in PLFE LUVETs (Figure 6A). This implies that the phytanyl chains and the saccharides (inositol in our case) may contribute (*9*, *12*, *33*, *34*), to some extent, to the remarkable low proton permeability and the high thermal stability in PLFE liposomes, but these two structural factors alone are not sufficient to generate the effects.

It is more important to note that proton permeabilities in DSPC LUVETs come close to those in PLFE LUVETs (Figure 6A). In fact, below the main phase transition temperature of DSPC (54.9 °C, *35*), the proton permeability in DSPC LUVETs is slightly lower than that in PLFE LUVETs. Numerous physical data have shown that lipid acyl chains in the gel state DSPC bilayers are highly ordered (e.g., *36*), and, molecular modeling (J. Gabriel, personal communication) and fluorescence probe (*7*) studies have shown that lipid packing in PLFE liposomes is unusually tight and rigid, especially at low temperatures. The similar *P* values for both PLFE LUVETs and gel-state DSPC LUVETs (Figure 6A) suggest that lipid packing in PLFE liposomes is a major contributor of the low proton permeation in PLFE LUVETs. This proposition is in line with the theory that proton permeation across lipid bilayers occurs through hydrated transient defects produced by thermal fluctuations or headgroup jumps (*34*, *37*, *38*). According to these permeation mechanisms, tight and rigid lipid packing should reduce transient defects, thus lowering proton permeability.

Figure 6A also shows that, above the transition temperature (54.9 °C), the proton permeation in DSPC LUVETs begins to increase with increasing temperature and becomes significantly higher than that in PLFE LUVETs. This observation can also be understood in terms of lipid packing. It is well known that the molecular packing of liquid−crystalline DSPC bilayers is loose, compared to gel-state DSPC bilayers. In contrast, PLFE liposomes lack a distinct phase transition in the temperature range examined, and the packing of PLFE liposomes remains relatively tight even at high temperatures (*7*). This difference in lipid packing between DSPC and PLFE may explain why the proton permeability in DSPC becomes significantly higher than that in PLFE above 54.9 °C.

Another possible contributing factor is the hydrocarbon chain length. Paula et al. (*39*) recently demonstrated that increasing the fatty acyl chain length reduces the proton permeation across the lipid bilayer. DSPC contains 18 carbons in its acyl chains; thus, the entire hydrocarbon region in the gel-state DSPC bilayer is 36 carbons long (assuming the methylene carbons are in *all-trans* configurations), which is somewhat longer than the phytanyl chains (32 carbons excluding the branched methyl carbons) in PLFE LUVETs. According to Paula et al. (*39*), this chain length difference would make the proton permeability in DSPC lower than that in PLFE LUVETs below the main phase transition temperature (54.9 °C) of DSPC. Above the transition temperature, the proton permeation in DSPC LUVETs begins to increase with increasing temperature and becomes significantly higher than that in PLFE LUVETs (Figure 6A). This phenomenon may be attributed to the presence of gauche conformations in the methylene carbons of liquid−crystalline DSPC bilayers and to the rigid structure of PLFE. Gauche conformations lead to the formation of kinks in the lipid acyl chains, which shorten the effective bilayer thickness. In contrast, PLFE does not possess any distinct phase transition and the phytanyl chains of PLFE span the entire membrane, lacking the mid-plane spacing. Such a structural rigidity would make the thickness of the PLFE hydrocarbon layer less temperature sensitive. Thus, it is conceivable that the difference in the thickness of the hydrocarbon layers between DSPC and PLFE may be reversed at the transition temperature of DSPC. This provides an alternative explanation for the higher proton permeability in DSPC above 54.9 °C. However, the DPhPC results (Figure 6A) argue against the idea that thickness of the hydrophobic region accounts for the low proton permeability across PLFE membranes because the lengths of the hydrophobic regions in both DPhPC and PLFE membranes are about the same (∼32 carbons long), yet the proton permeation in DPhPC is significantly higher than that in PLFE liposomes at any given temperature examined (Figure 6A). To this end, it can be concluded that tight and rigid lipid packing is still the most plausible explanation for the low proton permeability and its high thermostability in PLFE LUVETs.

Deamer and Nichols (*40*) demonstrated that the decay of large pH gradients across lipid bilayers produces a diffusion potential, limiting a new proton flux and consequently leading to an underestimation of proton permeability coefficient. To address this issue, we have conducted the proton permeability measurements of PLFE and eggPC in the presence of valinomycin and K^+ ions at a pH gradient of 1.0 (i.e., pH 7.0 in the interior and pH 6.0 in the bulk aqueous phase). Under these experimental conditions, the proton permeabilities in liposomes are indeed increased (Figure 6B), presumably due to the release of the diffusion potential. This result agrees with the previous finding that valinomycin acts as an ion carrier in the very unusual tetraether lipid membranes (*41*). However, in the presence of valinomycin, the proton permeability across PLFE membranes is still low and far less temperature sensitive compared with other liposomes (illustrated in Figure 6B).

Figure 7A shows that small PLFE liposomes (SUVETs, ∼60 nm in diameter) exhibit a lower proton permeability than large PLFE liposomes (LUVETs, ∼240 nm in diameter). More interestingly, the proton permeability in PLFE SUVETs is even less sensitive to temperature, changing by less than 2×10^{-10} cm/s from 25 to 82 °C, than that in PLFE LUVETs. The Arrhenius plots of the initial rate constant of proton permeation in PLFE LUVETs and PLFE SUVETs are linear (Figure 4B), with a higher activation energy for

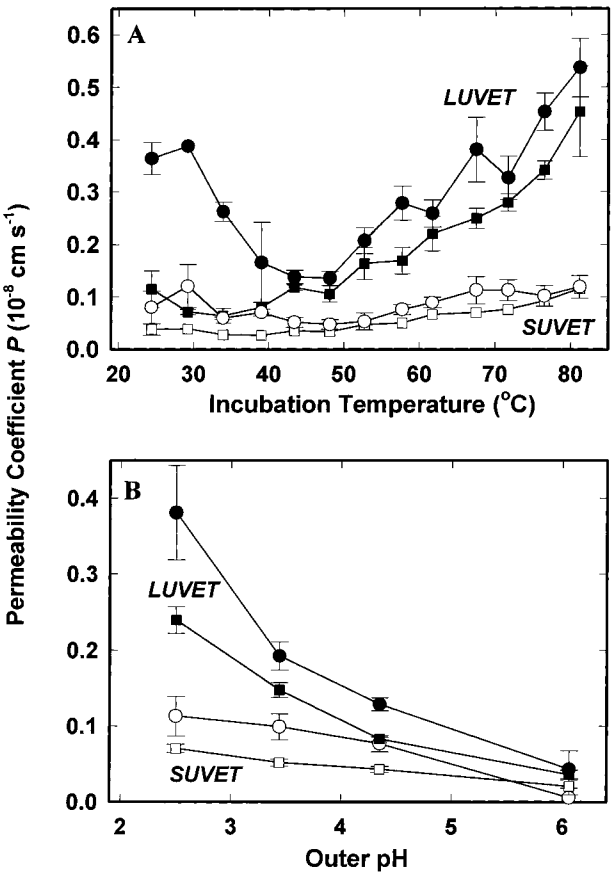

FIGURE 7: (A) Effect of temperature on apparent proton permeability coefficient P in PLFE LUVETs (filled symbols) and PLFE SUVETs (open symbols). (B) Effect of the initial pH in the bulk aqueous phase on apparent proton permeability ceofficient P in PLFE LUVETs (filled symbols) and PLFE SUVETs (open symbols) at 67.7 °C. The pH in the inner aqueous compartment at time zero was 7.0. Circles and squares were calculated from the initial proton permeation rate constant k_0 and the average rate constant $\langle k \rangle$, respectively.

PLFE SUVETs (6.7 kcal/mol vs 5.1 kcal/mol for PLFE LUVETs, Table 1). Figure 7B shows that the proton permeability coefficient P decreases with decreasing the magnitude of the initial pH gradient in both PLFE LUVETs and PLFE SUVETs, but the decreasing rate of P with the initial pH gradient is less dramatic in the case of PLFE SUVETs as opposed to PLFE LUVETs (Figure 7B). At present, the physical origin of the extremely low temperature sensitivity for proton permeability in PLFE SUVETs is not known. One possibility is that, when the vesicle diameter is reduced from ~240 to ~60 nm, the phosphate groups in PLFE liposomes may change from a random transmembrane distribution to a situation with a disproportionate amount of negatively charged phosphate localized to the outer surface, in a way similar to the asymmetric transbilayer redistribution of PG in small unilamellar vesicles previously reported by Michaelson et al. (*42*) and Lentz et al. (*43*). This transmembrane rearrangement may lead to a tighter lipid packing and, thus, a lower temperature sensitivity for proton permeation. In any case, the vesicle diameter effect (Figure 7) may be biologically relevant because the electron micrograph showed that the whole cell of *S. acidocaldarius* exhibits an irregular shape with a diameter of ~0.7−1.0 μm and that the cell surface is multilobed (*10*, *44*). The multilobed structure implies that highly curved membrane regions with the radius of curvature similar to that in PLFE SUVETs (~60 nm in diameter) are likely to exist in *S. acidocaldarius* and that these highly curved regions would be thermally stable in regard to proton permeability (Figure 7A).

In conclusion, our present data show that PLFE liposomes exhibit remarkable thermal stability in terms of 5(6)CF leakage and proton permeation. The low leakage rate of 5(6)CF can be attributed to the negative charges on membrane surface and the tight and rigid lipid packing. The tight and rigid lipid packing is also the major contributing factor of the low proton permeation found in PLFE liposomes. These findings provide a better understanding of the physiological role of archaebacterial membranes. The extremely high thermal stability in PLFE SUVETs (Figure 7A) is particularly appealing for applications in biotechnology such as sterilization and development of drug delivery liposomes and for the reconstitution study of channel-forming proteins or peptides (reviewed in ref 45).

ACKNOWLEDGMENT

We thank Dr. Eddie L. Chang for technical advice and Ms. Lihua Wei for assistance in the isolation of PLFE lipids from *S. acidocaldarius*, Dr. David W. Deamer for helpful discussions, and Dr. Satoshi Okada, Dr. Hiroyuki Saito, Mr. Hiromitsu Aoki, and Ms. Aya Kitajima for their support in the measurements of the sizes and the zeta-potentials of the liposomes.

REFERENCES

1. Lo, S.-L., and Chang, E. L. (1990) *Biochem. Biophys. Res. Commun. 167*, 238−243.
2. Langworthy, T. A. (1985) in *Archaebacteria VIII* (Woese, C. R., and Wolfe, R. S., Eds.) pp 459−498, Academic Press, New York, NY.
3. De Rosa, M., Gambacorta, A., and Gliozzi, A. (1986) *Microbiol. Rev. 50*, 70−80.
4. Kates, M. (1992) *Biochem. Soc. Symp. 58*, 51−72.
5. De Rosa, M., and Gambacorta, A. (1988) *Prog. Lipid Res. 27*, 153−175.
6. Elferink, M. G. L., de Wit, J. G., Demel, R., Driessen, A. J. M., and Knonings, W. N. (1992) *J. Biol. Chem. 267*, 1375−1381.
7. Kao, Y. L., Chang, E. L., and Chong, P. L.-G. (1992) *Biochem. Biophys. Res. Commun. 188*, 1241−1246.
8. Chang, E. L. (1994) *Biochem. Biophys. Res. Commun. 202*, 673−679.
9. Elferink, M. G. L., de Wit, J. G., Driessen, A. J. M., and Knonings, W. N. (1994) *Biochim. Biophys. Acta 1193*, 247−254.
10. Brock, T.D., Brock, K. M., Belly, R. T., and Weiss, R. L. (1972) *Arch. Mikrobiol. 84*, 54−68.
11. Choquet, C. G., Patel, G. B., Beveridge, T. J., and Sprott, G. D. (1994) *Appl. Microbiol. Biotechnol. 42*, 375−384.
12. Yamauchi, K., Doi, K., Yoshida, Y., and Kinoshita, M. (1993) *Biochim. Biophys. Acta 1146*, 178−182.
13. Hope, M. J., Bally, M. B., Webb, G., and Cullis, P. R. (1985) *Biochim. Biophys. Acta 812*, 55−65.
14. Frokjaer, S., Hjorth, E. L., and Worts, O. (1983) in *Liposome Technology* (Gregoriadis, G., Ed.) Vol. I, pp 235−246, CRC Press, Boca Raton, FL.
15. Bott, S. E. (1987) in *Particle Size Distribution* (Provder, T., Ed.) pp 74−88, American Chemical Society, Washington, DC.
16. Komatsu, H., Handa, T., and Okada, S. (1997) *J. Pharm. Sci. 86*, 497−502.
17. New, R. R. C. (1990) in *Liposomes: A Practical Approach* (New, R. R. C., Ed.) pp 105−160, Oxford University Press, New York, NY.

18. Bramhall, J., Hofmann, J., DeGuzman, R., Montestruque, S., and Schell, R. (1987) *Biochemistry 26*, 6330−6340.
19. Jorgensen, K., Ipsen, J. H., Mouritsen, O. G., Bennett, D., and Zuckermann, M. J. (1991) *Biochim. Biophys. Acta 1067*, 241−253.
20. Allen, T. M., and Cleland, L. G. (1980) *Biochim. Biophys. Acta 597*, 418−426.
21. Komatsu, H., and Okada, S. (1995) *Biochim. Biophys. Acta 1237*, 169−175.
22. Ohki, S., and Spangler, A. (1992) in *The Structure of Biological Membranes* (Yeagle, P., Ed.) pp 655−720, CRC Press, Boca Raton, FL.
23. Szoka, F. C., Jacobson, K., and Papahadjopoulos, D. (1979) *Biochim. Biophys. Acta 551*, 295−303.
24. Thomas, J. A., Buchsbaum, R. N., Zimniak, A., and Racker, E. (1979) *Biochemistry 18*, 2210−2218.
25. Barchfeld, G. L., and Deamer, D. W. (1985) *Biochim. Biophys. Acta 819*, 161−169.
26. Zeng, J., Smith, K. E., and Chong, P. L.-G. (1993) *Biophys. J. 65*, 1404−1414.
27. Norris, F. A., and Powell, G. L. (1990) *Biochim. Biophys. Acta 1030*, 165−171.
28. De Young, L. R., and Dill, K. A. (1988) *Biochemistry 27*, 5281−5289.
29. Spencer, G., Wei, L., and Chong, P. L.-G. (1993) *Biophys. J. 64*, A75.
30. Lindsey, H., Petersen, N. O., and Chan, S. I. (1979) *Biochim. Biophys. Acta 555*, 147−167.
31. Borle, F., and Seelig, J. (1983) *Biochemistry 22*, 5536−5544.
32. Vaz, W. L. C., Hallmann, D., Clegg, R. M., Gambacorta, A., and De Rosa, M. (1985) *Eur. Biophys. J. 12*, 19−24.
33. Gliozzi, A., Rolandi, R., De Rosa, M., and Gambacorta, A. (1983) *J. Membr. Biol. 75*, 45−56.
34. Haines, T. H. (1994) *FEBS Lett. 346*, 115−122.
35. Hinz, H.-J., and Sturtevant, J. M. (1972) *J. Biol. Chem. 247*, 6071−6075.
36. Yellin, N., and Levin, I. W. (1977) *Biochemistry 16*, 642−647.
37. Nagle, J. F., and Scott, H. L. (1978) *Biochim. Biophys. Acta 513*, 236−243.
38. Nichols, J. W., and Deamer, D. W. (1980) *Proc. Natl. Acad. Sci. U.S.A. 77*, 2038−2042.
39. Paula, S., Volkov, A. G., van Hoek, A. N., Haines, T. H., and Deamer, D. W. (1996) *Biophys. J. 70*, 339−348.
40. Deamer, D. W., and Nichols, J. W. (1983) *Proc. Natl. Acad. Sci. U.S.A. 80*, 165−168.
41. Gliozzi, A., Paoli, G., Rolandi, R., De Rosa, M., and Gambacorta, A. (1982) *J. Bioelectrochem. Bioenerg. 9*, 591−601.
42. Michaelson, D. M., Horwitz, A. F., and Klein, M. P. (1973) *Biochemistry 12*, 2637−2645.
43. Lentz, B. R., Alford, D. R., and Dombrose, F. A. (1980) *Biochemistry 19*, 2555−2559.
44. Lubben, M., and Schafer, G. (1987) *Eur. J. Biochem. 164*, 533−540.
45. Hsieh, C.-H., Sue, S.-C., Lyu, P.-C., and Wu, W. (1997) *Biophys. J. 73*, 870−877.

BI972163E